ACS OMEGA

http://pubs.acs.org/journal/acsodf

Article

Changes in Selected Organic and Inorganic Compounds in the Hydrothermal Carbonization Process Liquid While in Storage

Nader Marzban,* Judy A. Libra,* Vera Susanne Rotter, Kyoung S. Ro, Daniela Moloeznik Paniagua, and Svitlana Filonenko*

Cite This: *ACS Omega* 2023, 8, 4234−4243

Read Online

ACCESS | Metrics & More | Article Recommendations | Supporting Information

ABSTRACT: Although many studies have investigated the hydrothermal transformation of feedstock biomass, little is known about the stability of the compounds present in the process liquid after the carbonization process is completed. The physicochemical characteristics of hydrothermal carbonization (HTC) liquid products may change over storage time, diminishing the amount of desired products or producing unwanted contaminants. These changes may restrict the use of HTC liquid products. Here, we investigate the effect of storage temperature (20, 4, and −18 °C) and time (weeks 1−12) on structural and compositional changes of selected organic compounds and physicochemical characteristics of the process liquid from the HTC of digested cow manure. ANOVA showed that the storage time has a significant effect on the concentrations of almost all of the selected organic compounds, except acetic acid. Considerable changes in the composition of the process liquid took place at all studied temperatures, including deep freezing at −18 °C. Prominent is the polymerization of aromatic compounds with the formation of precipitates, which settle over time. This, in turn, influences the inorganic compounds present in the liquid phase by chelating or selectively adsorbing them. The implications of these results on the further processing of the process liquid for various applications are discussed.

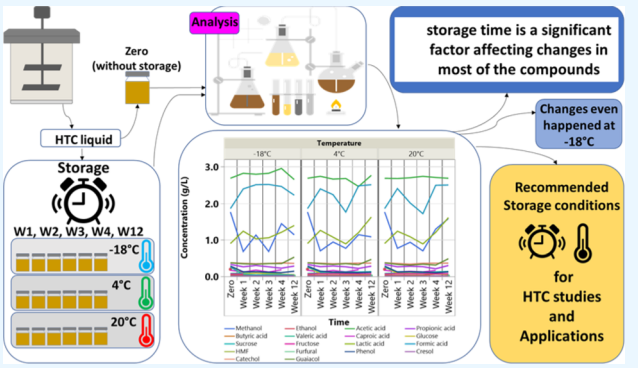

INTRODUCTION

Hydrothermal carbonization (HTC) is an emerging green technology, which can be used in process combinations to valorize waste streams in biorefineries and convert low-value wet biomass into value-added products such as a carbonaceous solid called hydrochar, and a process liquid containing a variety of organic compounds such as reducing sugars, alcohols, hydroxymethylfurfural (HMF), furfural, volatile fatty acid, organic acids,[1,2] and phenols.[3] The hydrochar can be used for various fuel,[4−6] soil,[7] and environmental applications.[8−10] While applications for the recovery of selected organic compounds from the liquid phase (e.g., HMF) for the production of a wide range of polymers and biofuels[11] show economic potential,[12] the remaining soluble compounds can be valorized through the production of biogas via anaerobic digestion.[13]

The spectrum and amount of organic compounds produced in the HTC reactions depend on the feedstock type and the process conditions (reaction temperature and time[3,14,15]). By following the formation of selected reaction products (five aromatics, four sugars, and three organic acids) in the process liquid as a function of HTC process conditions with three feedstocks, Reza et al.[3] reported large differences in the production and disappearance of the compounds over the reaction time. The wide range of compounds, their reactivity, and the complex matrix make the separation and identification of individual compounds difficult. Becker et al. found that 50%−90% of the total organic carbon (TOC) measured in the HTC process water for eight feedstocks was not accounted for after quantifying nine of the major organic components.[16]

The chemical composition of the HTC process liquid may also change after completion of the HTC treatment and during storage while waiting for the next downstream process, such as the extraction of certain chemicals or anaerobic digestion for biogas production. Reactive organic species formed in the hydrothermal treatment phase can still be present in the slurry at room temperature. Interactions between unreacted moieties and dissolved organic chemicals may occur throughout the cooling phase and in the postprocessing or handling steps at room temperature or even at lower temperatures since many of them are highly reactive and can quickly undergo polymer-

Received: November 18, 2022
Accepted: December 23, 2022
Published: January 19, 2023

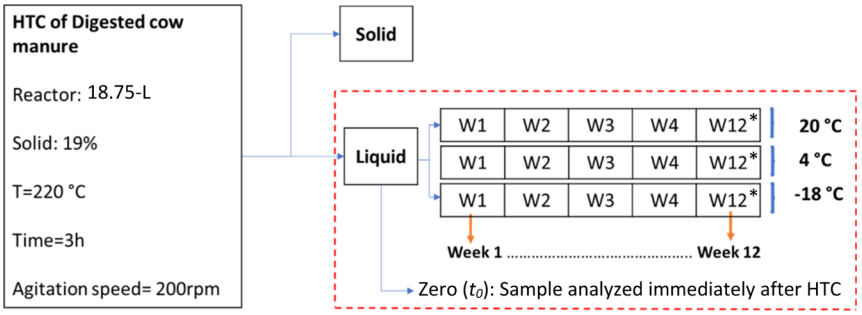

Figure 1. Scheme of the performed storage experiment.

ization with the formation of precipitates by condensation reactions.[17] A similar instability of bio-oils from the fast pyrolysis of lignocellulosic biomass, which often contains between 20 and 30% water, has been found.[18] Their behavior under storage with accelerated and long-term aging has been well studied due to their significance as renewable substitutes for conventional petroleum fuels.[18−21] Because of their high content of reactive oxygen-containing compounds, bio-oils under storage have been found to undergo polymerization and condensation reactions, resulting in the formation of water-insoluble products and increased viscosity.[19] Storage of filtered bio-oil under refrigeration at 5 °C was found to minimize changes in viscosity.[20] However, there is no data reported in the literature concerning changes in the physiochemical characteristics of the aqueous HTC process liquid while in storage. Such changes are of interest since reactions in the HTC process liquid after completion of HTC treatment can diminish the amount of desired products or can produce unwanted contaminants, restricting the uses of the HTC process liquid. This reactivity may affect the outcomes of HTC applications at full scale as well as in lab studies on reaction kinetics or process influences if not considered in the planning for downstream processing, handling, and storage.

This work is aimed at determining the quantitative and qualitative changes in the chemical composition and structures of the HTC process liquid while in storage. We investigated the effect of storage temperature (20, 4, and −18 °C) and time (weeks 1−12) on selected organic and inorganic compounds as well as physicochemical characteristics of the HTC process liquid by comparing the values measured over the 12 weeks period to that of the fresh HTC liquid. We also made recommendations for suitable storage temperatures and times to minimize the change in HTC process liquid characteristics.

EXPERIMENTAL SECTION

Hydrothermal Carbonization. The carbonization procedure was performed with digested cow manure slurry (pH = 8.3) obtained from a local biogas plant operating at a dairy farm. It was composed of 19% total solids (% S_o) and 81% liquid (wt %). The detergent fiber analysis of the feedstock was performed based on VDLUFA (2012; methods 6.5.1, 6.5.2, and 6.5.3)[22] and can be found in Table S1 of the Supporting Information. The feedstock slurry (12.007 kg fresh mass) was filled into an 18.75 L high-pressure reactor (5 gal, Model 4557, Parr Instrument Company, Moline, Illinois 61265-1770 USA). The reactor was sealed and heated to 220 °C at a rate of 2 K/min (temperature controller Model 4848BM, 6000-Watt 3-band heater) and held for 3 h at 220 °C. The heating, reaction, and cooling overnight were performed under constant mixing at 200 rpm. The cooled reaction mixture contained hydrochar and process liquid. The process liquid was separated from the solid char using vacuum filtration (ROTH filter 5−8 μm). The separated liquid was poured into at least three separate bottles (200 mL screw top filled with approximately 96 g) for analysis at each storage time and temperature. The experimental design with the number of bottles, the defined storage duration, and temperatures is outlined in Figure 1. A control (or zero-time sample t_0) was taken after the separation of the liquid phase from the solid products (1 h after opening the reactor), was immediately prepared for each analytical method, and then analyzed. The rest of the process liquid was stored for later analysis at −18, 4, and 20 °C, in a freezer, refrigerator, and climate chamber, respectively. Three samples from each bottle were analyzed for all analytical methods. The content of the storage bottles was homogenized by manual shaking prior to taking the three samples, except for W12, which is explained below. The storage duration plan was designed to have an analysis of the samples more often at the beginning of the storage period (each week in the first month: W1, W2, W3, and W4) based on the assumption that analysis is typically performed within 1 month after the production of carbonization products. The final sample time was 12 weeks (W12).

Analytical Methods for Product Characterization. The detailed sample preparation and analytical methods for each sample can be found in the Supporting Information (section Additional experimental details, materials, and methods). In brief, the individual compounds followed over time in the liquid samples were sugars (glucose, sucrose, and fructose), aromatics (phenol, cresol, catechol, guaiacol, furfural, and HMF), and organic acids (lactic and formic) measured by HPLC methods, alcohols, and fatty acids by GC methods, and inorganics by ICP-OES methods. The chemical oxygen demand (COD), pH, total organic carbon in liquid (TOC), total solids (TS %), and organic total solids (oTS %) were also measured. In addition, NMR, zeta potential, and dynamic light scattering (DLS) analyses were performed to study changes in the liquid over the 4 weeks of storage. The precipitates from W12 were characterized using XRD, FTIR, SEM, ICP-OES, and elemental analysis.

Separation of Natural Precipitates and Humic Acid at W12. During storage, precipitates were gradually formed in the pristine process liquid regardless of the storage temperature, visible as brown suspended solids settled at the bottom of the bottle. Small amounts of precipitates were observed already after only 1 week of storage, and storing the process liquid for 12 weeks resulted in the formation of a considerable amount of natural precipitates in samples stored at all three temperatures. At W12, an additional study of the precipitates was carried out with three bottles at each storage temperature (−18, 4, and 20

https://doi.org/10.1021/acsomega.2c07419
ACS Omega 2023, 8, 4234−4243

Table 1. Mean Value and Standard Deviation of Selected Organic Compounds, Ash %, TOC, COD, TS %, oTS %, and pH of the HTC Process Liquid Sample Zero at t_0 Prior to Storage

sugars (g/L)	aromatics (g/L)	organic acids (g/L)	alcohols (g/L)	lumped parameters
fructose = 0.06 ± 0.002	catechol = 0.37 ± 0.017	acetic = 2.69 ± 0.11	ethanol = 0.19 ± 0.03	ash % = 1.34 ± 0.04
glucose = 0.25 ± 0.011	cresol = 0.09 ± 0.0007	butyric = 0.03 ± 0	methanol = 1.76 ± 0.47	COD (g/L) = 45.18 ± 0.21
sucrose = 0.25 ± 0.01	furfural = BDL[a]	caproic = 0.17 ± 0.011		oTS % = 1.95 ± 0.05
	guaiacol = 0.370 ± 0.022	formic = 1.85 ± 0.02		pH = 7.4 ± 0.01
	HMF = 0.002 ± 0.0002	lactic = 0.89 ± 0.16		TOC (g/L) = 15.88 ± 0.01
	phenol = 0.279 ± 0.09	propionic = 0.33 ± 0.02		TS % = 3.29 ± 0.13
		valeric = 0.08 ± 0.006		

[a]BDL means that the furfural concentration was below the detection limit of the instrument.

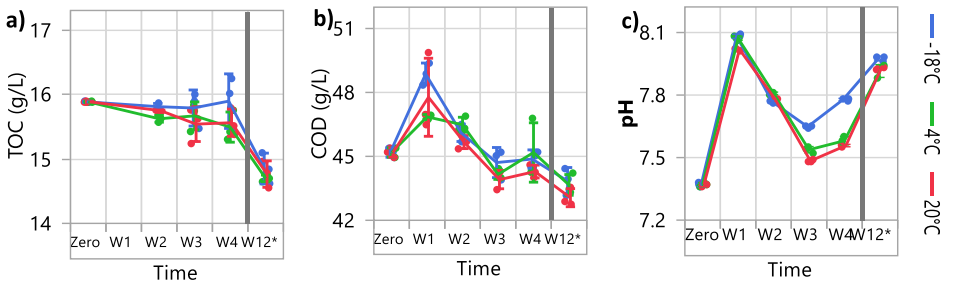

Figure 2. Effect of storage conditions of the process liquid on (a) the TOC#, (b) COD, and (c) pH (#due to a technical problem, TOC could not be measured at W1. For W12*, the brown natural precipitate was removed by centrifugation before measurement).

°C); more details are given in the Supporting Information. Samples were taken of the supernatants and/or precipitates: (1) after the bottle content was homogenized and the precipitate removed by centrifugation (W12*; precipitates stored at −18, 4, 20 °C: W12P1, W12P2, and W12P3), (2) after the bottle content was acidified to precipitate humic acid (HA) and both precipitates (HA and natural) removed by centrifugation (precipitates stored at −18, 4, 20 °C: W12PA1, W12PA2, and W12PA3), which here we called HA. The weight percentage of the total precipitates for each storage temperature was determined. The liquid and solid samples were analyzed as stated in the analytical section above and in the supplementary methods.

Statistical Data Analysis. Every analysis was repeated at least in triplicate (depending on the instrument and method) for each sample bottle over the storage time (see Table S2 in the Supporting Information). The data are reported as mean value ± standard deviation. We used JMP14 from SAS to identify the significant difference between the values (p-value ≤ 0.05) measured for the stored samples and to see if the data is statistically different from the values measured immediately after the HTC experiment, the zero-time value t_0, using the ANOVA and Dunnett's test, respectively. The summary of statistical data analysis is provided in Tables S3−S5 (in the Supporting Information).

RESULTS AND DISCUSSION

Composition of the Process Liquid. The initial concentrations of important individual organic compounds (sugars, aromatics, organic acids, and alcohols) and lumped parameters (TOC, COD, TS %, oTS %, and pH) found in the process liquid after the HTC production run at zero time t_0 are summarized in Table 1. The values for the total and organic solids in the process liquid (3.29 TS %, 59.27 oTS %) measured directly after separation from the hydrochar by filtration show that organic compounds make up almost 60% of the 32.9 g/L of dissolved compounds found. As expected, the process liquid contains high amounts of organic acids, mainly acetic and formic acids (2.69 and 1.85 g/L, respectively), and methanol (1.76 g/L). The phenolic compounds catechol and guaiacol are the main aromatics present, both at 0.37 g/L, while glucose and sucrose were both measured at 0.25 g/L. This is surprising since glucose, which is produced from the hydrolysis of cellulose in the HTC process, usually undergoes the isomerization reaction to form fructose and can directly undergo fragmentation and dehydration reactions to form HMF and furfural.[23−25] 5-HMF was produced in low amounts in the HTC of the cow digestate, while other aromatic compounds, namely, guaiacol, catechol, and phenol, were found to be formed from the hydrolysis and dealkylation of dissolved lignin in a homogeneous reaction in HTC.[26] Guaiacol has been determined as an initial degradation product of lignin in the liquid[27] and, together with catechol, represents the most common aromatic compounds in the mixture. Previous works reported that organic acids were formed from xylose, furfural, and retro-aldol products,[28] glucose,[29,30] fructose,[31] and their formation reduces the pH of the process liquid and facilitates further reaction of intermediates, such as dehydration of glucose to HMF.[32,33] Here, the formation of organic acids during the HTC process was not sufficient to lower the reaction medium pH into acidic conditions; therefore, it resulted in the lower formation of HMF. In addition, according to the fiber analysis of feedstock (Table S1 in the Supporting Information), the cow manure digestate comprised 19.27, 2.27, and 21.34% of cellulose, hemicellulose, and lignin, respectively. The low content of cellulose and high content of lignin in feedstock after anaerobic digestion resulted in minor production of HMF and furfural, whereas a significant production of lignin-derived aromatic compounds was formed in the process liquid, respectively. Alcohols are produced from the decarboxylation of amino acids and fatty acids in the HTC process.[34]

A comparison of the TOC analyzed in the process liquid (15.88 g/L) to the sum of the organic carbon quantified in the

https://doi.org/10.1021/acsomega.2c07419
ACS Omega 2023, 8, 4234−4243

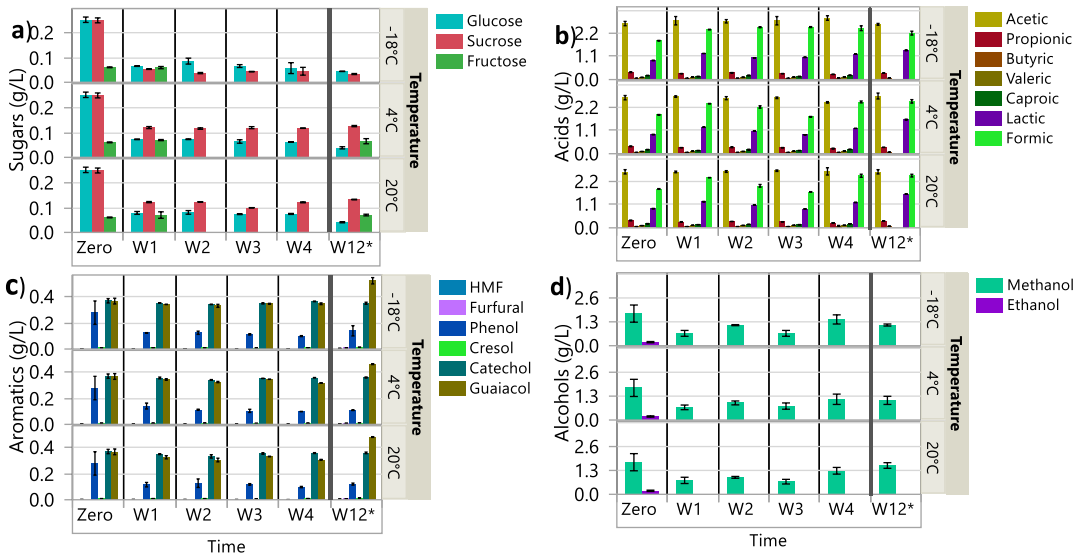

Figure 3. Change in the concentrations of the organic compounds in the hydrothermal process liquid over the 12 weeks of storage time, from right after the reactor opening (zero) to samples stored at −18, 4, and 20 °C for 12 weeks: (a) sugars, (b) organic acids, (c) aromatics, and (d) alcohols. (Figures for each individual compound can be found in Figure S2 of the Supporting Information.) (For W12*, the brown natural precipitate was removed by centrifugation before measurement.)

individual compounds shows that only 24.8% of the TOC is accounted for. Subsequent analysis of the process liquid at W12 for HA indicated that an additional 11.2% of the TOC could be associated with the group of HA. These results are similar to those reported by Becker et al. 2014 for eight lignocellulosic feedstocks, in which only 10−50% of the TOC measured could be accounted for after nine of the major individual organic components were quantified by GC and HLPC.[16] However, the selected dissolved organic compounds (e.g., sugars, organic acids, and aromatics) play a crucial role in the HTC process,[3,32,35] mainly in the formation of spherical-like secondary hydrochar, which condenses on the surface of primary hydrochar.[36]

Changes in the Lumped Parameters of the Process Liquid over Storage Time. The changes in the TOC and COD concentrations and pH over the 12 weeks of storage time are shown in Figure 2 compared to the zero-time values for the three different temperatures. Little to no change in TOC concentration was found in the homogenized samples over the 12 weeks, remaining close to the high initial value, 15.88 g/L. Visual changes in the samples took place during storage; brown suspended solids that settled at the bottom of the bottle were gradually formed in the pristine process liquid regardless of the storage temperature. These precipitates are often attributed to the polymerization and precipitation of organic compounds.[36] They appeared after only 1 week of storage and grew to considerable amounts over the 12 weeks. However, compared to zero time, removal of the precipitates in the samples at W12 by centrifugation showed that only 1.03, 1.18, and 1.08 g/L of TOC was associated with the precipitates (respectively for −18, 4, and 20 °C). The quantity and characteristics of the precipitate at week 12 are discussed in detail in the section precipitates and HA below. As Figure 2b,c shows, there were changes in the degree of oxidation of the compounds in the liquids as measured by COD as well as in the pH over the storage time. These changes may result from continuing decomposition reactions. The COD increased by up to 48.86, 46.85, and 47.77 g/L after the first week, and then decreased again to 46.1, 46.48, and 45.67 g/L and after removal of the precipitate decreased to 43.84, 43.66, and 43.06 g/L, for the samples at −18, 4 and 20 °C, respectively.

The pH of samples changed with a similar trend over the storage time regardless of storage temperature (Figure 2c). The biggest increase in pH initially might result from two factors: (1) the degassing of the CO_2 dissolved in liquid once the liquid was exposed more to the atmospheric pressure; (2) the precipitation of anions which, is discussed more in detail. There were no significant trends in the TS % over 4 weeks of storage, however; at week 12, the TS was significantly reduced after the removal of precipitates (Figure S1). The lowest ash content (wt %) was measured at week 12, after the removal of precipitates.

Changes in the Organic Compounds in the Process Liquid over Storage Time. Storing the sample leads to a significant decrease in glucose and sucrose at all three temperatures (Figure 3a). This large decrease occurred during the first week of sample storage. Thereafter, the concentrations remained relatively constant. Fructose concentrations rapidly dropped to below the detection limit (0.02 g/L) after week 1, though some were detected again in week 12 at 4 and 20 °C. The largest decrease in all three sugars came surprisingly at −18 °C compared to 4 and 20 °C. At week 12, the amount of sugars is the lowest at −18 °C. We observed a small amount of a very dark liquid accumulated above the ice surface at −18 °C. This accumulation might increase the availability of different organic fragments, for example, sugars, to participate in reactions with other molecules.

Most of the decreases in sugars may be due to the formation of organic acids, with very small amounts undergoing the dehydration reactions to form HMF and furfural. This is indicated by the behavior of the individual acids in Figure 3 over storage time. For example, Figure 3b shows the amount of formic acid increased while glucose decreased significantly in week 1. Then, the amount of formic acid significantly decreased (from weeks 1 to 3) at temperatures of 4 and 20 °C, although at −18 °C, it remained almost constant. The increase in formic acid during the first week may be explained by the oxidation of glucose to formic acid and CO_2;[37] then

https://doi.org/10.1021/acsomega.2c07419
ACS Omega 2023, 8, 4234−4243

(from weeks 1 to 3), the formic acid may have decomposed to form CO_2.[38,39] Similarly, the lactic acid concentration increased during the first week of storage, which corresponds to the decrease in the glucose concentration. As seen in Figure 2c, the pH increased during the first week of storage. The increase in pH is known to facilitate the conversion of glucose to lactic acid,[40] which is explained by the autoneutralizing formation of carboxylate groups by retro-aldol addition from the sugars.[40,41] Further variations in the lactic acid concentration may be connected to polycondensation reactions together with furan derivatives to form the humic condensate.[41] In contrast, the storage conditions and time had little effect on the acetic acid concentration, and it remained almost constant over the 12 weeks. Similar behavior was reported for acetic acid during the storage of pyrolysis bio-oil.[19] Although there were some significant differences for some of the other fatty acids (e.g., propionic, valeric, caproic acids; Table S5) between the values at the six storage times measured, there were no clear trends over time.

For the five-membered aromatic heterocycles, HMF and furfural, the storage time and temperature had no significant effect on their concentrations in the first 4 weeks (Figure 3c). Only a small amount of furfural was measured in the zero time, and it decreased below the detection limit (0.02 mg/L) from weeks 1 to 4. In week 12, both increased, although remaining at low levels of approximately 4−5 mg/L (HMF) and 8 mg/L (furfural).

The phenolic compounds showed some variations over storage time, but little difference between the storage temperatures. The trends of the individual compounds were varied: while the phenol concentration decreased over the 12 weeks of storage time, the cresol and guaiacol concentrations were increased at W12 compared to the zero-time values. However, the changes in concentrations did not follow consistent trends. The amount of guaiacol and catechol decreased gradually during 2 weeks of storing the sample and increased again at W3. The decrease in both compounds at 20 °C was higher than that for 4 and −18 °C. However, at week 12, the amount of guaiacol was approximately 30% higher than at zero time, while catechol was approximately the same as the beginning value. Guaiacol has also been reported to be unstable after 6-month storage in fast-pyrolysis bio-oil.[19] The storage condition had no significant effect on cresol concentration, which increased during the storage time (∼50%) for all three temperatures. The amount of phenol was significantly decreased in the first week of storage at all temperatures and remained at approximately 1/2 of the initial concentration. There were no significant differences between the decreases in phenol concentration at different temperatures. Previous works have observed an extensive condensation of phenols during accelerated aging,[21] while others have seen no changes over 1 year of storage of fast-pyrolysis bio-oil.[19] An indication that some of the lost phenol and catechol were involved in the polymerization and formation of solids in the liquid phase can be gathered from the sample that was acidified to extract the HA. After acidification, the amount of phenol almost reached its zero-time value, and catechol increased above its initial value (Table S6). This is discussed in the next section.

The significant decrease in alcohols during the storage (Figure 3d) might be attributed to the volatilization losses through the seal. After zero time, the ethanol content was under the detection limit of the instrument (<0.02 g/L).

Natural Precipitates and HA. In this section, we report on two types of solids in the samples from week 12: (1) the natural precipitates, which were formed during storage (W12P1, W12P2, and W12P3), and (2) the solids containing both the natural precipitates and HA present in process liquid, which was precipitated after acidifying the process liquid to pH = 1 using concentrated HCl (W12PA1, W12PA2, and W12PA3). The extra step to quantify HA was taken because the presence of humic substances is of interest in water treatment, where they are of concern for removal,[42,43] and in soil amendment, where they can be very beneficial and, therefore, a targeted product for the HTC process.[44] The HA can be formed by polycondensation reactions of low-molecular-weight compounds (e.g., amino acids, sugars, and phenols) in an alkaline medium.[41,44,45] In this study, the feedstock was a semialkaline digested cow manure (pH = 8.3), and the final process liquid had a pH of 7.4. Since these conditions could lead to the formation of these macromolecules during the HTC process, we quantified the effect of storage conditions on the HA concentration (wt %) in the process liquid after 12 weeks.

As can be seen in Table 2, the higher storage temperature of 20 °C leads to the lowest formation of the natural precipitate

Table 2. wt % of the Natural Precipitate and HA in the Process Liquid at Week 12 for the Three Storage Conditions −18, 4, and 20 °C

name	storage temperature (°C)	percentages in liquid (wt %)
W12P1	−18	0.118 ± 0.001
W12P2	4	0.122 ± 0.002
W12P3	20	0.096 ± 0.001
W12PA1	−18	0.133 ± 0.004
W12PA2	4	0.236 ± 0.003
W12PA3	20	0.257 ± 0.014

in the sample (W12P3). In contrast, for the HA-containing precipitate, the samples stored at 20 and 4 °C (W12PA3 and W12PA2) contained almost twice the amount of precipitate as that at −18 °C, that is, 0.257 and 0.236%, compared to 0.133% at −18 °C. The analysis and visual appearance of the natural precipitates, which were formed during the storage, are shown in Figure 4. As can be seen, the color of the solids formed at 4 and 20 °C was darker than that of the precipitate formed at −18 °C (Figure 4b) and contained higher amounts of carbon, nitrogen, sulfur, and hydrogen than those at −18 °C (Figure 4a). A check on the amount of carbon recovered as precipitate compared to the loss of carbon measured by TOC over the 12 weeks of storage (Figure 2a) shows that only 24% can be explained by precipitation. The rest may be due to volatilization losses.

Although the ash content could not be determined because of the small sample size available, measurement of 12 individual inorganic compounds via ICP-OES showed that all three precipitates contained considerable amounts of inorganic elements, ranging from the highest amount of 19.84 wt % at −18 °C to 15.09 and 14.06 wt % at 4 °C and 20 °C (Table S7 in the Supporting Information). The elements Ca, Mg, P, Na, and K accounted for over 95% of the mass, with the precipitate at −18 °C containing the highest amount of P, Ca, and Mg (Figure 4d). It is possible that anions (e.g., P) and then cations (e.g., K) were chelated/adsorbed by the polymerized aromatics forming the precipitate. This can be

https://doi.org/10.1021/acsomega.2c07419
ACS Omega 2023, 8, 4234−4243

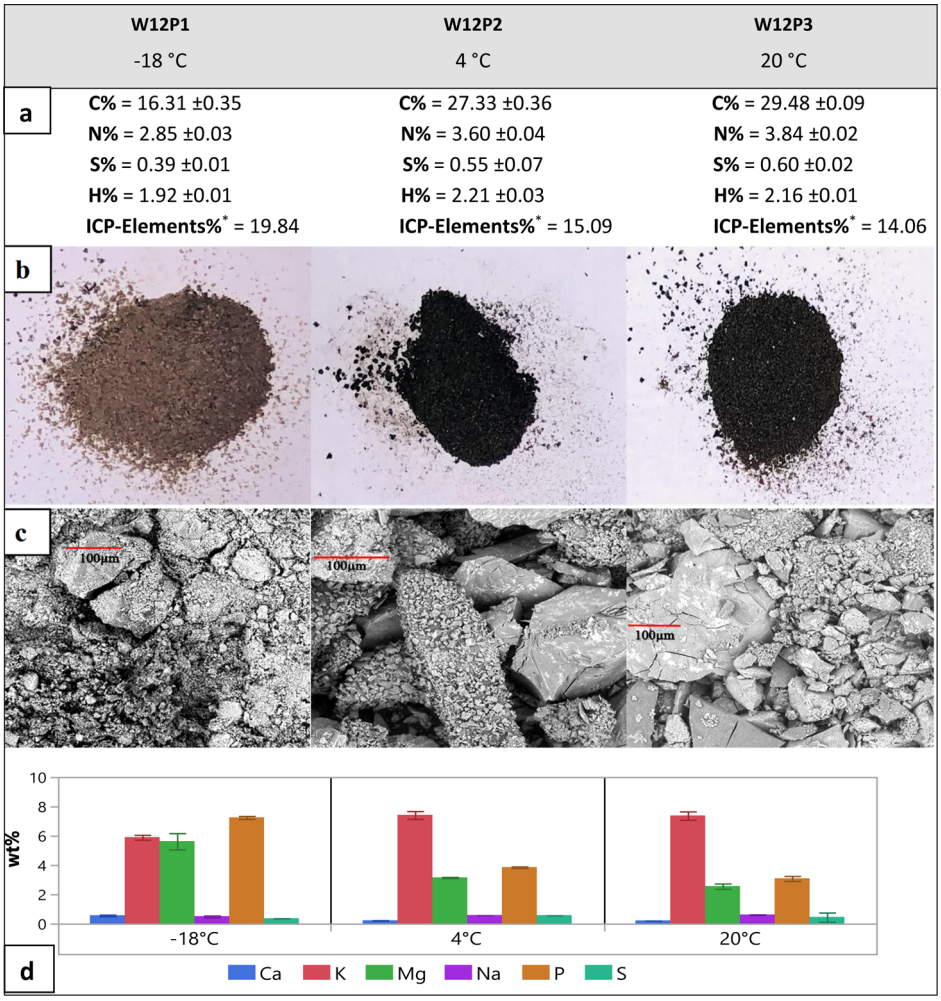

Figure 4. Compositional and physical characteristics of the natural precipitates at week 12 (W12P1-3) as (a) elemental analysis, (b) photos, (c) SEM images, and (d) ICP-OES wt %. [* means that it was calculated based on the sum of inorganics measured by ICP (excluding S %)].

supported by the change in pH values (Figure 2c). The high amount of inorganic compounds in the process liquid 1.34 wt % (ash content, Figure S1 in the Supporting Information) indicates the presence of a high number of ions that can participate in reactions.[46]

Characterization of the Precipitates. The HTC reaction produces highly reactive aromatic compounds, which continue to be polymerized even after heating has stopped. The condensed polymers can reach sizes in the nanoscale to microscale range. The nanoscaled particles pass through the filter in the separation step and can be detected already after the HTC. The color and turbidity of the process liquid change already upon the filtration (Figure S3, in the Supporting Information), indicating fast coalescence of the nanoparticles into sizes reaching hundreds of nanometers. Polymerization of the aromatic compounds formed as a result of hydrolysis during the HTC process, or later hydrolysis during storage, results in the constant appearance of particles with a size below nanometer, their coalescence into large aggregates, size growth, and eventual precipitation.

However, the abovementioned processes appear not to be sequential but rather to take place simultaneously. This is supported by the DLS analysis of the samples, revealing the presence of particles with three modes of size distribution already after the first storage week in the sample stored at room temperature (Figure S4a, in the Supporting Information). Obvious precipitates were formed at W12 of storage, which were separated and analyzed separately. Each sample has three types of particles of different sizes: particles 1, with a hydrodynamic diameter below 0.9 nm, particles 2 with a hydrodynamic diameter below 900 nm, and particles 3 with a hydrodynamic diameter below 1600 nm. The particles with a hydrodynamic diameter below 0.9 nm are present in all samples with a relatively similar size distribution between all storage temperatures over the storage time. The particles of type 2 are formed as aggregates of smaller particles, and there is more variability in the size between the samples. Particles 3 are the agglomerate with the largest hydrodynamic diameter observed in the samples stored at 20 °C.

The particles have a negative charge (Figure S4b, in the Supporting Information), and it is preserved over the storage experiment by changing the value. The charge of the polymer particles originates from carboxylic and phenolic groups, present in great abundance according to the data from the FTIR analysis. The freeze-dried samples were subjected to NMR analysis in order to define the functionality of the nanoparticles present in the process liquid (Figure S5 in the Supporting Information). The samples show the presence of aliphatic groups, abundance of hydroxide groups, carboxylic groups, and hydrogens in aromatic rings. The differences

https://doi.org/10.1021/acsomega.2c07419
ACS Omega 2023, 8, 4234−4243

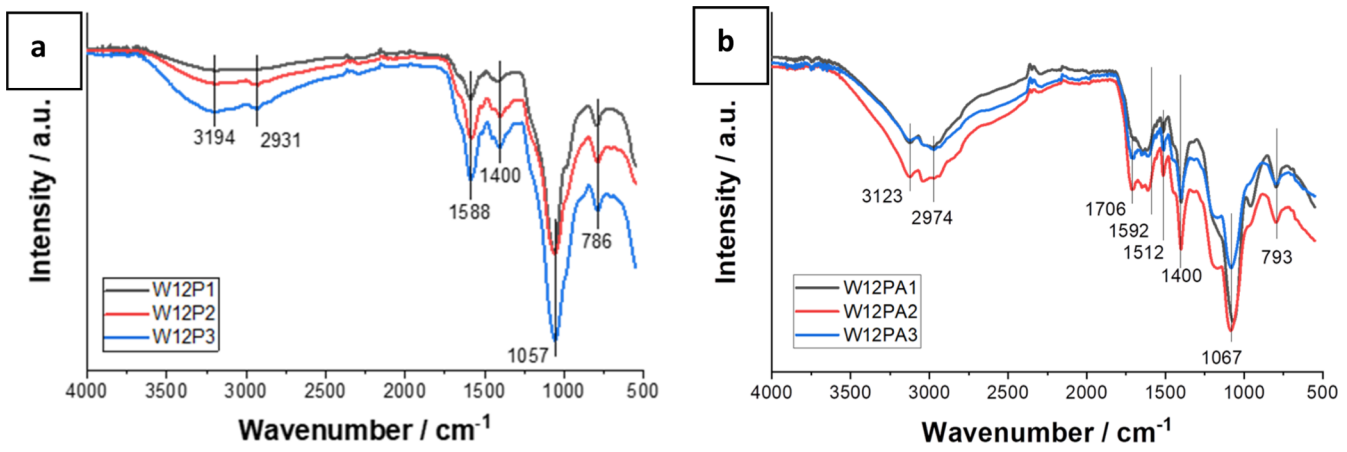

Figure 5. FTIR spectra of naturally precipitated solids during the storage period (a) and the HA (b).

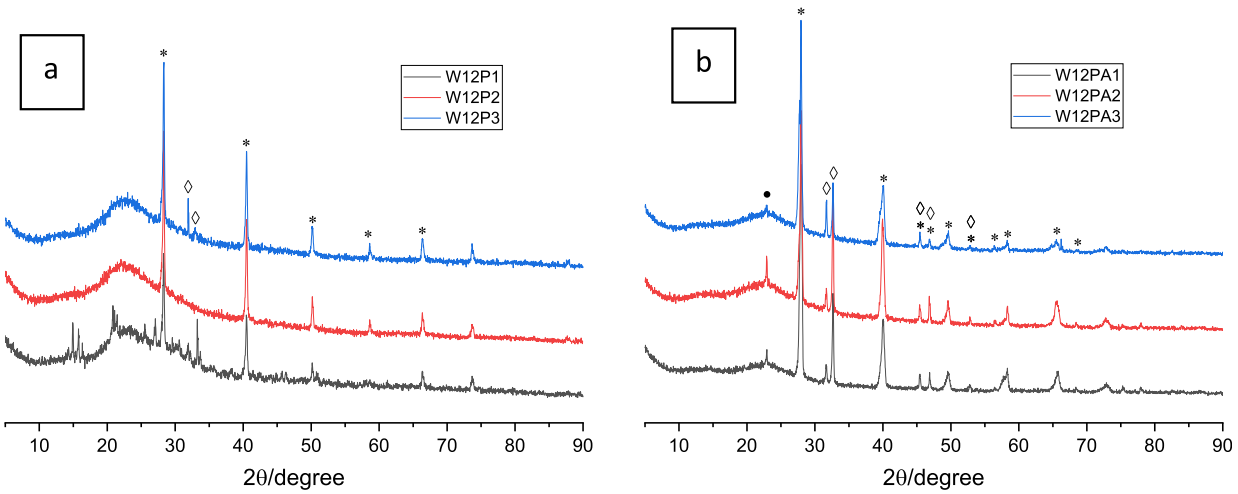

Figure 6. XRD of precipitated solids formed during the storage period (a) and HA (b): * corresponds to $K_3H(H_2P_2O_7)_2$ (96-210-7382); ◊ corresponds to $K_3HP_2O_6{\cdot}4H_2O$ (96-201-8714); ● corresponds to $K_6(P_6O_{12}){\cdot}8H_2O$ (96-153-4736).

between the FTIR analysis of the precipitates, which were formed in the liquid sample during the storage time, and those which were formed during the acidifications (HA) can be seen in Figure 5.

All three naturally formed precipitates have similar FTIR patterns independent of the storage temperature. Vibrational modes of the W12P sample are typical for hydrothermally obtained carbons: hydroxyl group broad band centered at 3194 cm^{-1}, stretching vibration of $-CH_x$ fragments as several bands in the range of 2800−3000 cm^{-1}; the band at 1588 cm^{-1} attributed to C═O asymmetric stretching and 1400 cm^{-1} attributed to C═C stretching; the strong band at 1057 cm^{-1} corresponds to C−O stretching in the primary C−O−H fragment of phenols. Notable that the intensity of the C═O stretching is higher than C═C, pointing to a lower degree of aromatization of the natural precipitates compared to hydrocarbons. The FTIR spectra of acidification precipitates contain bands of the same origin as the naturally formed precipitates; however, they exhibit several additional bands. Namely, the vibrational mode at 1706 cm^{-1} is referred to as C═O stretching in the carboxylic group and the band at 1512 cm^{-1} corresponds to N−H deformational vibration in the amide II group. The higher intensity of the 1400 cm^{-1} band compared to W12P samples presumes an abundance of phenol fragments in the W12PA samples.

The ICP analysis of the solids suggests large amounts of inorganic components in the naturally formed precipitates; namely, potassium and phosphorous, are the most common in all samples. This allows us to expect potassium phosphates as the main inorganic components of the precipitates. XRD analysis (Figure 6) identified three types of potassium phosphates in all samples, while the W12P1 sample contained an additional phase that was not identified and probably corresponds to mixed potassium−magnesium phosphates, which is supported by the higher content of Mg in the sample.

The XRD of the sample W12P1 has additional signals indicating the crystallization of more inorganic phases under storage at −18 °C. The storage temperature below the freezing temperature of water facilitates the crystallization of inorganic compounds. The XRD analysis reveals the presence of $CaHPO_4{\cdot}2H_2O$ with the signal at ca. 15 and $CaMg(CO_3)_2$ in accordance with the higher content of phosphorus, calcium, and magnesium.[47]

Recommended Storage Conditions. The results of the comparison between the values at time zero and the stored samples over the storage time and temperature show that (1) storage time is a significant factor affecting changes in most of

https://doi.org/10.1021/acsomega.2c07419
ACS Omega 2023, 8, 4234−4243

the compounds except for acetic acid and fructose and (2) significant changes occurred for most compounds at all three temperatures. Only furfural and acetic acid concentration changes were significantly dependent on the storage temperature. The dependence of the parameter changes on the storage time and temperatures was analyzed using a one-way ANOVA (Table S3 in the Supporting Information). Based on this and further statistical analysis (Tables S4 and S5 in the Supporting Information), the recommended storage temperature and maximum storage duration before analysis for each group of organic compounds are summarized in Table 3. For

Table 3. Summary of Recommended Storage Conditions in Order to Avoid Significant Changes Compared to Zero-Time Values[a]

group	compound	temperature (°C)	time (week)
sugars	glucose	no storage	no storage
	sucrose	no storage	no storage
	fructose	NA	NA
aromatics	HMF	−18 °C	3
	furfural	NA	NA
	phenol	no storage	no storage
	catechol	−18 °C	1
	guaiacol	−18 °C	1
	cresol	−18 °C	4
organic acids	acetic acid	−18 and 20 °C	12
	propionic acid	no storage	no storage
	butyric acid	−18 °C	4
	caproic acid	no storage	no storage
	valeric acid	−18 °C	3
	lactic acid	no storage	no storage
	formic acid	no storage	no storage
alcohols	methanol	no storage	no storage
	ethanol	NA	NA
COD	no storage	no storage	
TOC	−18 °C	4	

[a]NA means the data was not available to make the decision for storage.

example, glucose and sucrose concentrations in all stored samples, independent of storage temperature, were significantly different from their zero-time values; therefore, no storage is recommended for them. Similarly, the phenol concentration underwent a rapid decrease (around 50%), and no storage is recommended. For the rest of the individual aromatic compounds such as HMF, catechol, guaiacol, and cresol, a temperature of −18 °C is suggested.

Acetic acid was not statistically different from their zero time values at storage temperatures of −18 and 20 °C over 12 weeks. The concentration of propionic, caproic, lactic acid, and formic acid fluctuated significantly during the storage time at all the temperatures; therefore, we recommend an immediate analysis for them. For alcohols, it is recommended not to store the sample. The TOC can be analyzed for 4 weeks at −18 °C, while the COD needs to be measured without storage.

Because there was significant variation in the concentration of inorganics at the three temperatures and over time, it is recommended to avoid storage (Tables S8 and S9, Supporting Information). Further studies are needed to determine if preparing the samples immediately by acid digestion will preserve sample stability.

CONCLUSIONS

The physicochemical characteristics of HTC process liquid were found to change over time while in storage at all studied temperatures, including deep freezing at −18 °C. This reactivity must be taken into consideration in the planning of experiments to determine process kinetics and the influence of process conditions on liquid products. The recommendations above should help prioritize the analytical steps since some delays in processing samples are often unavoidable. Furthermore, these changes may affect the outcomes of full-scale HTC applications due to storage and handling between downstream processing steps. Since the HTC process is often operated in batch mode, the storage of process liquid is often necessary, so appropriate conditions need to be chosen for the intended application. For purposes of aromatic recovery in a biorefinery, the results of this study show that storage between process steps can affect the amount of compounds to be recovered. The highest amount of phenol and catechol was measured at time zero, while for HMF, furfural, guaiacol, and cresol, the highest was found at week 12. Transformation of the remaining sugars to HMF and furfural over storage time increased their concentrations. For the purpose of biogas production through anaerobic digestion, possible changes in inhibitor concentrations such as phenolic compounds[13,48] and light metal ions (e.g., Na, K, Mg, and Ca)[48] are of interest, along with any changes in potential substrate concentrations, measured as individual compounds or lumped parameters TOC or COD.[49,50] For example, improved biogas production may be expected for the process liquid stored for 12 weeks at 20 °C because phenol was significantly reduced, high amounts of light metals were precipitated, while the acetic acid remained almost unchanged, and the highest amounts of lactic and formic acids were observed. However, there was some loss in the potential substrate for biogas production, as evidenced by the drop in TOC and COD at week 12 due to the formation and removal of the precipitate and possible volatilization losses. Such trade-offs will need to be evaluated on a case-by-case basis for each feedstock and process combination. In general, due to the physicochemical instability of HTC liquid products in storage, it is recommended to perform pertinent analyses prior to its downstream processing and to match the storage conditions and expected changes to the goal of the applications.

ASSOCIATED CONTENT

Supporting Information

The Supporting Information is available free of charge at https://pubs.acs.org/doi/10.1021/acsomega.2c07419.

Additional experimental details, materials, and methods; statistical analysis; changes in TS %, oTS %, Ash %, and individual organic compounds; TOC and aromatic concentration of liquid after the precipitate removal, and ICP-OES analysis of precipitates; DLS, zeta potential, and NMR spectra of the process liquid; and changes in inorganics measured by ICP-OES and recommended storage conditions (PDF)

AUTHOR INFORMATION

Corresponding Authors

Nader Marzban − *Leibniz Institute of Agricultural Engineering and Bio-economy e.V. (ATB), 14469 Potsdam, Germany; Department of Environmental Technology, Chair of Circular*

https://doi.org/10.1021/acsomega.2c07419
ACS Omega 2023, 8, 4234−4243

Economy and Recycling Technology, Technische Universität Berlin, 10623 Berlin, Germany; Department of Colloid Chemistry, Max-Planck Institute of Colloids and Interfaces, 14476 Potsdam, Germany; orcid.org/0000-0001-7787-7706; Email: nmarzban@atb-potsdam.de

Judy A. Libra − *Leibniz Institute of Agricultural Engineering and Bio-economy e.V. (ATB), 14469 Potsdam, Germany;* Email: jlibra@atb-potsdam.de

Svitlana Filonenko − *Department of Colloid Chemistry, Max-Planck Institute of Colloids and Interfaces, 14476 Potsdam, Germany;* orcid.org/0000-0001-6888-877X; Email: Svitlana.Filonenko@mpikg.mpg.de

Authors

Vera Susanne Rotter − *Department of Environmental Technology, Chair of Circular Economy and Recycling Technology, Technische Universität Berlin, 10623 Berlin, Germany;* orcid.org/0000-0001-9300-7292

Kyoung S. Ro − *USDA-ARS, Coastal Plains Soil, Water & Plant Research Center, Florence, South Carolina 29501, United States*

Daniela Moloeznik Paniagua − *Leibniz Institute of Agricultural Engineering and Bio-economy e.V. (ATB), 14469 Potsdam, Germany; Department of Environmental Technology, Chair of Circular Economy and Recycling Technology, Technische Universität Berlin, 10623 Berlin, Germany*

Complete contact information is available at: https://pubs.acs.org/10.1021/acsomega.2c07419

Notes

The authors declare no competing financial interest.

■ ACKNOWLEDGMENTS

We thank the German Academic Exchange Service (DAAD) for providing financial support and the analytical chemistry group (Leibniz Institute of Agricultural Engineering and Bioeconomy) for their expertise and support with the analytical techniques. This research was supported by the United States Department of Agriculture (USDA), Agricultural Research Service (ARS), and National Programs 212 Soil. The mention of trade names or commercial products in this publication is solely for the purpose of providing specific information and does not imply recommendation or endorsement by the USDA.

■ REFERENCES

(1) Deng, C.; Lin, R.; Kang, X.; Wu, B.; Ning, X.; Wall, D.; Murphy, J. D. Co-Production of Hydrochar, Levulinic Acid and Value-Added Chemicals by Microwave-Assisted Hydrothermal Carbonization of Seaweed. *Chem. Eng. J.* **2022**, *441*, 135915.

(2) Nakason, K.; Panyapinyopol, B.; Kanokkantapong, V.; Viriya-empikul, N.; Kraithong, W.; Pavasant, P. Characteristics of Hydrochar and Hydrothermal Liquid Products from Hydrothermal Carbonization of Corncob. *Biomass Convers. Biorefin.* **2018**, *8*, 199−210.

(3) Reza, M. T.; Wirth, B.; Lüder, U.; Werner, M. Behavior of Selected Hydrolyzed and Dehydrated Products during Hydrothermal Carbonization of Biomass. *Bioresour. Technol.* **2014**, *169*, 352−361.

(4) Ro, K. S.; Flora, J. R. V.; Bae, S.; Libra, J. A.; Berge, N. D.; Álvarez-Murillo, A.; Li, L. Properties of Animal-Manure-Based Hydrochars and Predictions Using Published Models. *ACS Sustainable Chem. Eng.* **2017**, *5*, 7317−7324.

(5) Ro, K. S.; Libra, J. A.; Bae, S.; Berge, N. D.; Flora, J. R. V.; Pecenka, R. Combustion Behavior of Animal-Manure-Based Hydrochar and Pyrochar. *ACS Sustainable Chem. Eng.* **2019**, *7*, 470−478.

(6) Marzban, N.; Libra, J. A.; Hosseini, S. H.; Fischer, M. G.; Rotter, V. S. Experimental Evaluation and Application of Genetic Programming to Develop Predictive Correlations for Hydrochar Higher Heating Value and Yield to Optimize the Energy Content. *J. Environ. Chem. Eng.* **2022**, *10*, 108880.

(7) Puccini, M.; Ceccarini, L.; Antichi, D.; Seggiani, M.; Tavarini, S.; Hernandez Latorre, M.; Vitolo, S. Hydrothermal Carbonization of Municipal Woody and Herbaceous Prunings: Hydrochar Valorisation as Soil Amendment and Growth Medium for Horticulture. *Sustainability* **2018**, *10*, 846.

(8) Jian, X.; Zhuang, X.; Li, B.; Xu, X.; Wei, Z.; Song, Y.; Jiang, E. Comparison of Characterization and Adsorption of Biochars Produced from Hydrothermal Carbonization and Pyrolysis. *Environ. Technol. Innovation* **2018**, *10*, 27−35.

(9) Ferrentino, R.; Ceccato, R.; Marchetti, V.; Andreottola, G.; Fiori, L. Sewage Sludge Hydrochar: An Option for Removal of Methylene Blue from Wastewater. *Appl. Sci.* **2020**, *10*, 3445.

(10) Kohzadi, S.; Marzban, N.; Libra, J. A.; Bundschuh, M.; Maleki, A. Removal of RhB from Water by Fe-Modified Hydrochar and Biochar—An Experimental Evaluation Supported by Genetic Programming. *J. Mol. Liq.* **2023**, *369*, 120971.

(11) Pereira, A.; Woodman, T. J.; Chuck, C. J. An Integrated Biorefinery to Produce 5-(Hydroxymethyl)Furfural and Alternative Fuel Precursors from Macroalgae and Spent Coffee Grounds. *Sustainable Energy Fuels* **2021**, *5*, 6189−6196.

(12) Isemin, R.; Muratova, N.; Kuzmin, S.; Klimov, D.; Kokh-Tatarenko, V.; Mikhalev, A.; Milovanov, O.; Dalibard, A.; Ibitowa, O. A.; Nowotny, M.; Brulé, M.; Tabet, F.; Rogge, B. Characteristics of Hydrochar and Liquid Products Obtained by Hydrothermal Carbonization and Wet Torrefaction of Poultry Litter in Mixture with Wood Sawdust. *Processes* **2021**, *9*, 2082.

(13) Wirth, B.; Mumme, J. Anaerobic Digestion of Waste Water from Hydrothermal Carbonization of Corn Silage. *Appl. Bioenergy* **2014**, *1*, 1.

(14) Becker, R.; Dorgerloh, U.; Helmis, M.; Mumme, J.; Diakité, M.; Nehls, I. Hydrothermally Carbonized Plant Materials: Patterns of Volatile Organic Compounds Detected by Gas Chromatography. *Bioresour. Technol.* **2013**, *130*, 621−628.

(15) Chen, C.; Liang, W.; Fan, F.; Wang, C. The Effect of Temperature on the Properties of Hydrochars Obtained by Hydrothermal Carbonization of Waste *Camellia oleifera* Shells. *ACS Omega* **2021**, *6*, 16546−16552.

(16) Becker, R.; Dorgerloh, U.; Paulke, E.; Mumme, J.; Nehls, I. Hydrothermal Carbonization of Biomass: Major Organic Components of the Aqueous Phase. *Chem. Eng. Technol.* **2014**, *37*, 511−518.

(17) Funke, A.; Ziegler, F. Hydrothermal Carbonization of Biomass: A Summary and Discussion of Chemical Mechanisms for Process Engineering. *Biofuels, Bioprod. Biorefin.* **2010**, *4*, 160−177.

(18) Alsbou, E.; Helleur, B. Accelerated Aging of Bio-Oil from Fast Pyrolysis of Hardwood. *Energy Fuels* **2014**, *28*, 3224−3235.

(19) Oasmaa, A.; Kuoppala, E. Fast Pyrolysis of Forestry Residue. 3. Storage Stability of Liquid Fuel. *Energy Fuels* **2003**, *17*, 1075−1084.

(20) Elliott, D. C.; Oasmaa, A.; Meier, D.; Preto, F.; Bridgwater, A. V. Results of the IEA Round Robin on Viscosity and Aging of Fast Pyrolysis Bio-Oils: Long-Term Tests and Repeatability. *Energy Fuels* **2012**, *26*, 7362−7366.

(21) Black, S.; Ferrell, J. R. Accelerated Aging of Fast Pyrolysis Bio-Oil: A New Method Based on Carbonyl Titration. *RSC Adv.* **2020**, *10*, 10046−10054.

(22) *VDLUFA Handbuch. Der Landwirtschaftlichen Versuchs-Und Untersuchungsmethodik (VDLUFA-Methodenbuch)*. (Bd. III. Die Chemische Untersuchung von Futtermitteln); VDLUFA Verlag: Darmstadt, 2012.

(23) Sevilla, M.; Fuertes, A. B. The Production of Carbon Materials by Hydrothermal Carbonization of Cellulose. *Carbon* **2009**, *47*, 2281−2289.

(24) Sevilla, M.; Fuertes, A. B. Chemical and Structural Properties of Carbonaceous Products Obtained by Hydrothermal Carbonization of Saccharides. *Chem. Eur. J.* **2009**, *15*, 4195−4203.
(25) Falco, C.; Perez Caballero, F.; Babonneau, F.; Gervais, C.; Laurent, G.; Titirici, M.-M.; Baccile, N. Hydrothermal Carbon from Biomass: Structural Differences between Hydrothermal and Pyrolyzed Carbons via ^{13}C Solid State NMR. *Langmuir* **2011**, *27*, 14460−14471.
(26) Fang, Z.; Sato, T.; Smith, R. L.; Inomata, H.; Arai, K.; Kozinski, J. A. Reaction Chemistry and Phase Behavior of Lignin in High-Temperature and Supercritical Water. *Bioresour. Technol.* **2008**, *99*, 3424−3430.
(27) Pińkowska, H.; Wolak, P.; Złocińska, A. Hydrothermal Decomposition of Alkali Lignin in Sub- and Supercritical Water. *Chem. Eng. J.* **2012**, *187*, 410−414.
(28) Paksung, N.; Matsumura, Y. Decomposition of Xylose in Sub- and Supercritical Water. *Ind. Eng. Chem. Res.* **2015**, *54*, 7604−7613.
(29) Poerschmann, J.; Weiner, B.; Koehler, R.; Kopinke, F.-D. Hydrothermal Carbonization of Glucose, Fructose, and Xylose—Identification of Organic Products with Medium Molecular Masses. *ACS Sustainable Chem. Eng.* **2017**, *5*, 6420−6428.
(30) Demir-Cakan, R.; Baccile, N.; Antonietti, M.; Titirici, M.-M. Carboxylate-Rich Carbonaceous Materials via One-Step Hydrothermal Carbonization of Glucose in the Presence of Acrylic Acid. *Chem. Mater.* **2009**, *21*, 484−490.
(31) Asghari, F. S.; Yoshida, H. Kinetics of the Decomposition of Fructose Catalyzed by Hydrochloric Acid in Subcritical Water: Formation of 5-Hydroxymethylfurfural, Levulinic, and Formic Acids. *Ind. Eng. Chem. Res.* **2007**, *46*, 7703−7710.
(32) Hoekman, S. K.; Broch, A.; Robbins, C. Hydrothermal Carbonization (HTC) of Lignocellulosic Biomass. *Energy Fuels* **2011**, *25*, 1802−1810.
(33) Falco, C.; Baccile, N.; Titirici, M. Green Chemistry Morphological and Structural Differences between Glucose, Cellulose and Lignocellulosic Biomass Derived Hydrothermal Carbons. *Green Chem.* **2011**, *13*, 3273−3281.
(34) Liu, H.; Basar, I. A.; Nzihou, A.; Eskicioglu, C. Hydrochar Derived from Municipal Sludge through Hydrothermal Processing: A Critical Review on Its Formation, Characterization, and Valorization. *Water Res.* **2021**, *199*, 117186.
(35) Köchermann, J.; Görsch, K.; Wirth, B.; Mühlenberg, J.; Klemm, M. Hydrothermal Carbonization: Temperature Influence on Hydrochar and Aqueous Phase Composition during Process Water Recirculation. *J. Environ. Chem. Eng.* **2018**, *6*, 5481−5487.
(36) Lucian, M.; Volpe, M.; Gao, L.; Piro, G.; Goldfarb, J. L.; Fiori, L. Impact of Hydrothermal Carbonization Conditions on the Formation of Hydrochars and Secondary Chars from the Organic Fraction of Municipal Solid Waste. *Fuel* **2018**, *233*, 257−268.
(37) Voß, D.; Ponce, S.; Wesinger, S.; Etzold, B. J. M.; Albert, J. Combining Autoclave and LCWM Reactor Studies to Shed Light on the Kinetics of Glucose Oxidation Catalyzed by Doped Molybdenum-Based Heteropoly Acids. *RSC Adv.* **2019**, *9*, 29347−29356.
(38) Yu, J.; Savage, P. E. Decomposition of Formic Acid under Hydrothermal Conditions. *Ind. Eng. Chem. Res.* **1998**, *37*, 2−10.
(39) Berl, E.; Schmidt, A. Über das Verhalten der Cellulose bei der Druckerhitzung mit Wasser. *Justus Liebigs Ann. Chem.* **1928**, *461*, 192−220.
(40) Esposito, D.; Antonietti, M. Chemical Conversion of Sugars to Lactic Acid by Alkaline Hydrothermal Processes. *ChemSusChem* **2013**, *6*, 989−992.
(41) Yang, F.; Antonietti, M. Artificial Humic Acids: Sustainable Materials against Climate Change. *Adv. Sci.* **2020**, *7*, 1902992.
(42) Maleki, A.; Seifi, M.; Marzban, N. Evaluation of Sonocatalytic and Photocatalytic Processes Efficiency for Degradation of Humic Compounds Using Synthesized Transition-Metal-Doped ZnO Nanoparticles in Aqueous Solution. *J. Chem.* **2021**, *2021*, 9938579.
(43) Hasani, G.; Maleki, A.; Daraei, H.; Ghanbari, R.; Safari, M.; McKay, G.; Yetilmezsoy, K.; Ilhan, F.; Marzban, N. A Comparative Optimization and Performance Analysis of Four Different Electrocoagulation-Flotation Processes for Humic Acid Removal from Aqueous Solutions. *Process Saf. Environ. Prot.* **2019**, *121*, 103−117.
(44) Yang, F.; Antonietti, M. The Sleeping Giant: A Polymer View on Humic Matter in Synthesis and Applications. *Prog. Polym. Sci.* **2020**, *100*, 101182.
(45) Tkachenko, V.; Marzban, N.; Vogl, S.; Filonenko, S.; Antonietti, M. Chemical Insight into the Base-Tuned Hydrothermal Treatment of Side Stream Biomasses. *Sustainable Energy Fuels* **2023**, DOI: 10.1039/D2SE01513G.
(46) Reza, M. T.; Lynam, J. G.; Uddin, M. H.; Coronella, C. J. Hydrothermal Carbonization: Fate of Inorganics. *Biomass and Bioenergy* **2013**, *49*, 86−94.
(47) Wang, T.; Liu, H.; Duan, C.; Xu, R.; Zhang, Z.; She, D.; Zheng, J. The Eco-Friendly Biochar and Valuable Bio-Oil from *Caragana korshinskii*: Pyrolysis Preparation, Characterization, and Adsorption Applications. *Materials* **2020**, *13*, 3391.
(48) Chen, Y.; Cheng, J. J.; Creamer, K. S. Inhibition of Anaerobic Digestion Process: A Review. *Bioresour. Technol.* **2008**, *99*, 4044−4064.
(49) Michaud, S.; Bernet, N.; Buffière, P.; Roustan, M.; Moletta, R. Methane Yield as a Monitoring Parameter for the Start-up of Anaerobic Fixed Film Reactors. *Water Res.* **2002**, *36*, 1385−1391.
(50) Heidrich, E. S.; Curtis, T. P.; Dolfing, J. Determination of the Internal Chemical Energy of Wastewater. *Environ. Sci. Technol.* **2011**, *45*, 827−832.